Bistability of the Te donor in AlSb:Te bulk crystals

W. Jost,* M. Kunzer, and U. Kaufmann
Fraunhofer Institut für Angewandte Festkörperphysik, Tullastraße 72, D-79108 Freiburg, Federal Republic of Germany

H. Bender
Max-Planck-Institut für Festkörperforschung, Heisenbergstraße 1, D-70569 Stuttgart, Federal Republic of Germany
(Received 4 April 1994)

Photoenhanced electron-paramagnetic-resonance (EPR) and contactless photoconductivity measurements on Te-doped AlSb bulk crystals are reported. Low-temperature annealing studies of both photo-EPR and persistent photoconductivity strongly support a bistable *DX*-type model for the Te donor in AlSb and provide information on the deep *DX*-type state of Te.

I. INTRODUCTION

AlSb is attracting increasing attention because of its high potential for applications in heterostructure devices. The large conduction-band offset in AlSb/InAs heterojunctions and the small effective electron mass in InAs are very promising for transistor[1,2] and tunneling[3,4] device applications. The preferred *n*-type dopant for AlSb is Te. Wilkening *et al.*[5] presented magnetic resonance results for AlSb. An electron-paramagnetic-resonance (EPR) signal in AlSb:Te with a *g* value of 1.878 was identified as the shallow Te donor. A persistent photoenhancement of this signal was observed, but could not be explained unambiguously. Two possible explanations for this enhancement exist: First, photoneutralization of compensated donor-acceptor pairs, an effect that would be a property of the whole crystal; and second, a *DX*-type[6,7] change in the Te donor configuration associated with an electron transfer from the deep *DX* state to the shallow donor state. In this case photoenhancement would be a property of the dopant itself. The investigations to be reported here were performed to distinguish these two models. The results strongly support the *DX*-type model, i.e., a bistable behavior of the Te donor in AlSb.

II. EXPERIMENTAL DETAILS

The two bulk AlSb:Te crystals used for this study were grown by the Czochralski technique from a tellurium-doped melt.[8] The net donor concentration as determined by room-temperature Hall measurements is $(5-8)\times10^{17}$ cm^{-3} for sample 1 and 7×10^{16} cm^{-3} for sample 2.

The EPR measurements were performed at 9.5 GHz using 100-kHz field modulation and lock-in detection at temperatures between 5 and 125 K. Photoexcitation was achieved with a quartz-tungsten halogen lamp and interference filters. The lamp current was adjusted to maintain a constant photon flux at each wavelength. A mechanical shutter was used to define exposure times.

The photoconductivity of the crystals was measured contact free via the microwave absorption of the photogenerated free carriers. For this purpose sample 2 was mounted into the cavity of a *K*-band (18–26 GHz) optically detected magnetic-resonance setup, and the cavity was critically coupled in the dark. The contactless measurement of the conductivity is based on the fact that optically generated charge carriers induce a microwave absorption of the sample. This absorption causes a change in impedance of the cavity which in turn results in a change of the microwave power reflected from the cavity. This change in reflected microwave power was taken as measure for the photoconductivity.

III. RESULTS

Both samples reveal a Te shallow donor EPR signal already in the dark. Figure 1 shows the photoenhancement of this signal as a function of photon energy (full circles). Each data point corresponds to the initial slope $(\Delta I/\Delta t)_{t=0}$ of the EPR signal intensity transient I at the given photon energy. Therefore, the curve in Fig. 1 is

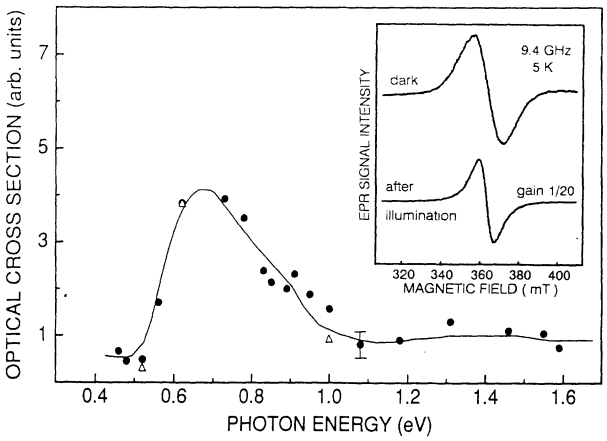

FIG. 1. Optical cross section as a function of photon energy of both photo-EPR (filled circles, 5 K) and PPC (open triangles, 70 K). The data of both measurements are normalized to each other at a photon energy of 0.6 eV. The full curve is a guide to the eye. The inset shows the EPR spectrum of AlSb:Te before and after *in situ* illumination.

proportional to an optical-absorption cross section. The photoenhancement persists when the light is switched off. The threshold for persistent enhancement is seen to be about 0.5 eV.

The neutral shallow donor concentrations were obtained from EPR by comparison with a GaP:S standard.[9] In the dark they are about 5×10^{16} cm^{-3} and below 10^{16} cm^{-3} for samples 1 and 2, respectively. Following enhancement with $h\nu=0.6$ eV light the concentration saturates at values of about 4×10^{17} and 4.5×10^{16} cm^{-3} for samples 1 and 2, respectively. Thus the increase in neutral shallow donors is about 3.5×10^{17} cm^{-3} in sample 1 and about 4×10^{16} cm^{-3} in sample 2.

An isochronal annealing study of the photoenhanced EPR signal was performed. The sample was first illuminated at 5 K with $h\nu\cong0.6$ eV light until the enhancement had saturated. The sample was then annealed for 12 min at temperatures between 70 and 125 K. Subsequently it was cooled to 5 K and the EPR spectrum was recorded again. The annealing curve thus obtained is shown in Fig. 2. It can be seen that the enhanced EPR signal intensity is thermally stable up to about 90 K, and decays to the dark intensity above that temperature.

A characteristic feature of *DX* centers is the phenomenon of persistent photoconductivity (PPC), i.e., a photoconductivity that persists when the light is switched off. Therefore we measured the photoconductivity of sample 2 via the contactless technique described in Sec. II. At 1.5 K, PPC was not observed with $h\nu=0.6$ eV excitation. However, the PPC is observed at 70 K. Photoconductivity transients were measured for three characteristic photon energies, and two of them are shown in Fig. 3. Their initial slopes are plotted in Fig. 1 as open triangles normalized such that the $h\nu=0.6$ eV data points matches the photo-EPR enhancement curve.

To study the low-temperature annealing behavior of PPC, we first saturated the photoconductivity optically at 70 K and then, in the dark, heated the sample to 140 K at a rate of 1 K/min. The conductivity was measured during the warm-up; see the full circles and the full curve in Fig. 4. It is seen to decay partially between 100 and 120 K, but increases again at higher temperatures. The sample was held for 5 min at 140 K and then cooled again. Down to 120 K the conductivity values fall onto the warm-up curve. However, below 120 K the conductivity (dashed curve) is smaller than during warm-up, and at 70 K reaches the original dark value.

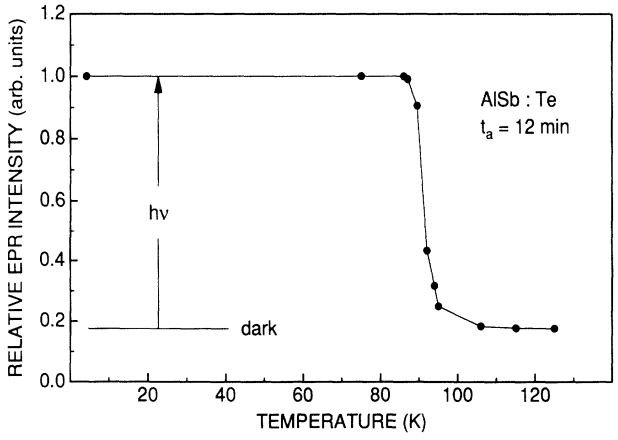

FIG. 2. Isochronal annealing of the photoenhanced ($h\nu=0.6$ eV) shallow donor EPR. The full curve is a guide to the eye.

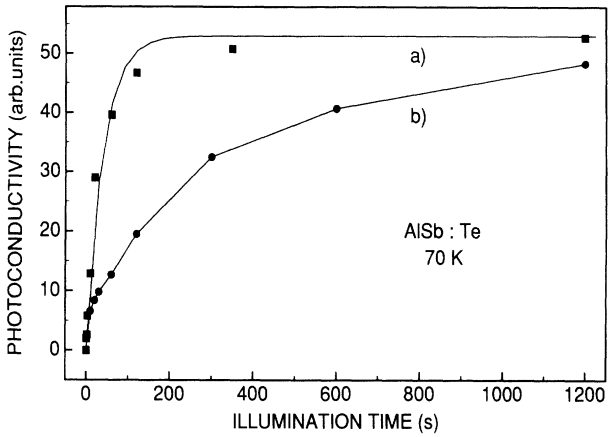

FIG. 3. Photoconductivity as a function of illumination time for a photon energy of 0.6 (a) and 0.5 eV (b).

IV. DISCUSSION

The light-induced increase of the shallow donor EPR signal results from an increase in *neutral* shallow donor centers. This means that electrons are transferred from an electron source to empty shallow donor states by the light. The similarity of the EPR enhancement curve and PPC data points in Fig. 1 strongly suggests that both experiments monitor the same electron transfer process. The only difference is that at 5 K, where EPR is observed, all electrons are frozen out at the shallow donors,

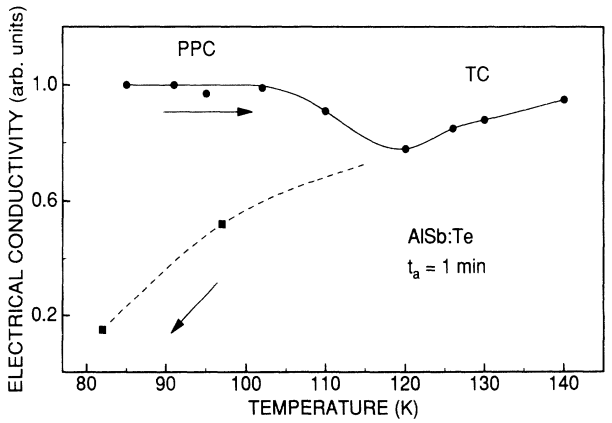

FIG. 4. Isochronal annealing of the PPC in AlSb:Te. The full curve connecting the full circles is the warm-up curve. The subsequently measured cool-down curve is identical with the warm-up curve above 120 K, and below that temperature corresponds to the dashed curve.

whereas at 70 K and above, where PPC is observed, the shallow donors are partially ionized. The main point now to be discussed is the source of electrons. This can be a deep acceptor level filled with electrons (compensation model), or a deep *DX*-type level of the Te donor itself (bistability model).

An explanation of the photo-EPR and the photoconductivity data within the compensation model would require a deep acceptor level about 0.5 eV below the conduction band, or even deeper, corresponding to the low-energy threshold in Fig. 1. According to the photoenhanced shallow donor concentrations quoted in Sec. II, the concentrations of this acceptor would be around 3.5×10^{17} cm^{-3} for sample 1 and around 4×10^{16} cm^{-3} for sample 2. Although an $(E_C-0.5)$-eV acceptor level cannot be definitely excluded by the present measurements, it is unlikely that its concentration varies by an order of magnitude in crystals which have been grown under virtually identical conditions.

It is also a problem to explain the photo-EPR annealing data in Fig. 2 within a simple compensation model. The annealing curve was analyzed by assuming that the photogenerated portion P of the EPR signal decays, at a fixed temperature T, according to $P=P_0\exp(-ct)$, where t is the annealing time and $c=c_0\exp(-E_a/kt)$ is a thermally activated decay rate. The parameter E_a is the activation energy for photo-EPR decay. The data points were transformed into an Arrhenius plot ln$c$ vs $1/T$ and E_a was obtained from the slope of the straight line through the data points. It was found that $E_a=(315\pm60)$ meV, i.e., considerably larger than the known Te shallow donor ionization energy $E_D=68$ meV.[10] This shows that the photo-EPR decay process involves not simply E_D but an additional barrier energy E_B such that $E_a=E_D+E_B$ with $E_B=(247\pm60)$ meV. Such behavior is unexpected for a normal shallow donor in a simple compensation model. Finally this model would not account for the observed PPC in Fig. 4.

We now proceed to discuss the results in a conventional *DX* picture, since the negative-*U* model for the *DX* centers is still under debate.[11] Bistable behavior of donors, where the donor can exist in two different defect configurations, one giving rise to a shallow level and the other to a deep level, has been known to occur in ternary III-V alloys for many years.[6,7] However, such behavior has been invoked only recently for binary III-V compounds, namely GaSb:S (Ref. 12) and AlSb:Te.[13] In the *DX* picture the source of electrons required to explain the photo-EPR and PPC data is a deep donor state at E_C-E_{DX} of the Te dopant itself; see the configuration coordinate model in Fig. 5. When a sample is slowly cooled to liquid-He temperatures in the dark, free electrons can be captured into the shallow donor level or in the deep *DX* level. In the present case the EPR data reveal that only about 10% of conduction electrons are captured into the shallow level. The relative equilibrium occupation at low temperatures can now be changed by light, i.e., an electron can be transferred optically from the *DX* level to an empty shallow donor level. In the *DX* picture this is the mechanism accounting for the photoenhancement of the shallow donor EPR, as originally suggested for the Si donor in $Al_xGa_{1-x}As$.[14] For the corresponding enhancement of the Te shallow donor EPR in $Al_xGa_{1-x}As$ the same process was suggested.[15] The quantum-mechanical threshold energy for this optical process in Fig. 5 is simply E_{DX}. Thus from the low-energy threshold in Fig. 1 one would estimate $E_{DX}\approx0.5$ eV. Very likely this value for E_{DX} is too large for several reasons: near $h\nu=0.5$ eV and below the photo-EPR data become unreliable because of absorption due to quartz components in the photo-EPR system. Second, if the DLTS (deep-level transient spectroscopy) data[16,17] for Te in $Al_xGa_{1-x}Sb$ $(0.5\le x\le0.7)$ are extrapolated to AlSb, for the DLTS emission energy E_e of the Te *DX* level in AlSb, one expects $E_e=E_{DX}+E_B\approx0.5$ eV. With $E_B\approx250$ meV as evaluated from Fig. 2, this means that E_{DX} must be smaller than 0.5 eV. Finally the conductivity data to be discussed below indicate the same. Nakagawa *et al.* observed a deep level with $E_e=0.26$ eV in epitaxial AlSb:Te, and ascribed it to the Te *DX* level. This relatively small value of E_e is difficult to reconcile with the present results and with those reported for $Al_xGa_{1-x}Sb$:Te.[16,17]

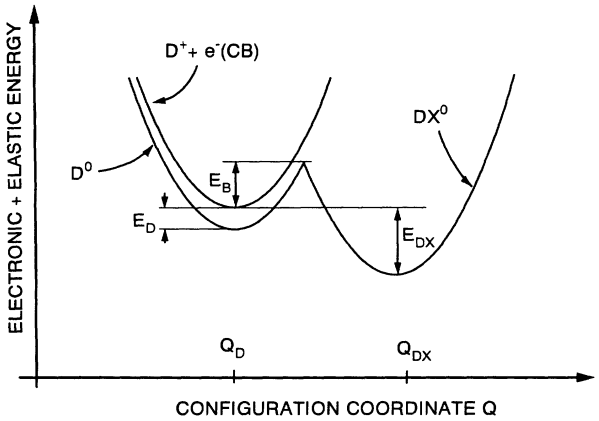

FIG. 5. Conventional (positive-*U*) configuration coordinate model used to describe the bistable behavior of the Te donor in AlSb. The shallow donor configuration D^0 is a metastable excited state of the deep DX^0 configuration.

After optical excitation of the electron from the *DX* level to the conduction band the electron is captured into the shallow level and remains there at LHe temperatures. Therefore, the photoenhanced portion of the EPR signal is stable when the light is switched off. If the temperature is now raised, thermal retransfer of the electron over the barrier in Fig. 5 will occur, and the EPR intensity will finally drop to the original dark value. The thermal activation energy for this decay is not simply E_D but $E_a=E_D+E_B$. The large E_a value inferred from Fig. 2 is thus explained by the *DX* model in a natural way.

The *DX* model also provides a simple explanation for the observed PPC. When electrons are excited optically from the *DX* level to the conduction band, at temperatures sufficiently low to prevent thermal retransfer over the barrier in Fig. 5 but high enough such that they are not completely frozen out at the shallow donor levels, there is a fraction of photoexcited electrons that give rise

to PPC. The fact that PPC was not observed at 1.5 K but was observed at 70 K shows that PPC is thermally activated. Actually the activation energy for PPC should be E_D. We have not attempted to confirm this, but the fact that PPC is observed at 70 K, i.e., well below the temperature range where photo-EPR decays (90–105 K), shows that the activation energy of PPC is smaller than $E_a = E_D + E_B$. The thermal decay characteristic of PPC should be the same as that of the photo-EPR. In the warm-up curve of Fig. 4, PPC is seen to decay in the range 100–115 K, i.e., at temperatures above the photo-EPR decay range. This is almost certainly due to the fact that the effective anneal time in Fig. 4 is an order of magnitude shorter than that in Fig. 2. Above 120 K the conductivity in the warm-up curve increases. Following the 5-min anneal at 140 K the conductivity in the subsequent cool-down falls onto the warm-up curve between 120 and 140 K, indicating that PPC has decayed completely above 120 K and that the conductivity is purely thermally induced in this range. This suggests that above 120 K the Te *DX* level is partially ionized and contributes to the conductivity. Below 120 K efficient carrier freeze-out at the *DX* level occurs.

Finally we want to show that the photoenhanced concentrations of *neutral* shallow Te donors quoted in Sec. III are consistent with the *DX* picture. In this model the concentration enhancement is proportional to the net Te donor concentration and therefore to the free-electron concentration at room temperature quoted in Sec. II for the two samples investigated. In fact, the ratio of concentration enhancement and free-electron concentration is around 0.5 in both samples. Taken together, all experimental results for the Te donor in AlSb are in line with the bistability model.

V. SUMMARY

We have presented photo-EPR and contact-free photoconductivity data for two different AlSb:Te bulk crystals as well as low-temperature annealing studies of these photogenerated signals. The result cannot be understood in a simple compensation model, whereas all observed features are naturally accounted for in a *DX*-type bistability model. We conclude that Te in AlSb is a bistable donor. This is a convincing example for such a donor in a binary III-V compound.

ACKNOWLEDGMENTS

We thank K. Sambeth for expert technical assistance, J. Schneider for useful comments on the manuscript, and W. Wilkening for his cooperation in taking early data as well as for useful discussions. This work has been supported in part by the German Bundesministerium für Forschung und Technologie (BMFT).

*Present address: Max-Planck-Institut für Festkörperforschung, Heisenbergstraße 1, D-70569 Stuttgart, Federal Republic of Germany.

[1]G. Tuttle, H. Kroemer, and J. H. English, J. Appl. Phys. **65**, 5239 (1989).

[2]L. F. Luo, R. Beresford, and W. I. Wang, Appl. Phys. Lett. **55**, 789 (1989).

[3]L. Yang, J. F. Chen, and A. Y. Cho, J. Appl. Phys. **68**, 2997 (1990).

[4]J. R. Soderström, E. R. Brown, C. D. Parker, L. J. Mahoney, J. Y. Yao, T. G. Anderson, and T. C. McGill, Appl. Phys. Lett. **58**, 275 (1991).

[5]W. Wilkening, U. Kaufmann, J. Schneider, E. Schönherr, E. R. Glaser, D. V. Shanabrook, J. R. Watermann, and R. J. Wagner, in *Material Science Forum*, edited by G. Davies, G. DeLeo, and M. Stavola (Trans Tech, Aedermansdorff, 1992), Vols. 83-87, p. 793.

[6]P. M. Mooney, J. Appl. Phys. **67**, R1 (1990).

[7]G. D. Watkins, in *Material Science Forum*, edited by G. Ferenczi (Trans Tech, Aedermansdorff, 1989, Vols. 38-41, p. 39.

[8]C. T. Lin, E. Schönherr, and H. Bender, J. Cryst. Growth **104**, 653 (1980).

[9]U. Kaufmann and T. A. Kennedy, J. Electron. Mater. **10**, 347 (1981).

[10]B. T. Ahlburn and A. K. Ramdas, Phys. Rev. **167**, 717 (1968).

[11]S. Subramanian, S. Anand, B. M. Arora, Y. C. Lu, and E. Bauser, Phys. Rev. B **48**, 8757 (1993).

[12]I. Poole, M. E. Lee, I. R. Cleverly, A. R. Peaker, and K. E. Singer, Appl. Phys. Lett. **57**, 1645 (1990).

[13]A. Nakagawa, J. J. Pekarik, H. Kroemer, and J. H. English, Appl. Phys. Lett. **57**, 1551 (1990).

[14]P. M. Mooney, W. Wilkening, U. Kaufmann, and T. F. Keuch, Phys. Rev. B **39**, 5554 (1989).

[15]H. J. v. Bardeleben, M. Zazoui, S. Alaya, and P. Gibart, Phys. Rev. B **42**, 1500 (1990).

[16]B. K. Meyer, G. Bischopink, K. W. Benz, A. Schöner, and G. Pensl, J. Cryst. Growth **128**, 475 (1993).

[17]Y. Zhu, T. Takeda, and A. Sasaki, J. Appl. Phys. **64**, 1897 (1988).